Sustainable Marine Structures
https://journals.nasspublishing.com/index.php/sms

ARTICLE

Predictive Modelling of Dynamic Positioning Vessel Capacity on Offshore Wind Industry

Nijalingappa Yogeesh [1*] , ***Suleiman Ibrahim Shelash Mohammad*** [2,3] , ***Natarajan Raja*** [4] , ***Asokan Vasudevan*** [5,6,7] , ***Thirumalesha Babu Tumkur Rangaswamy*** [8] , ***Ashalatha Kodihalli Siddagangaiah*** [9] , ***Anber Abraheem Mohammad*** [10]

[1] *Department of Mathematics, Government First Grade College, Badavanahalli-572112, Madhugiri Taluk, Tumakuru District, Karnataka 560001, India*

[2] *Department of Electronic Marketing and Social Media, Faculty of Economic and Administrative Sciences, Zarqa University, Zarqa 13110, Jordan*

[3] *Department of Business and Communications, INTI International University, Persiaran Perdana BBN, Putra Nilai 71800, Negeri Sembilan, Malaysia*

[4] *Department of Visual Communication, Sathyabama Institute of Science and Technology, Chennai, Tamil Nadu 600001, India*

[5] *Faculty of Business and Communications, INTI International University, Persiaran Perdana BBN, Putra Nilai 71800, Negeri Sembilan, Malaysia*

[6] *Faculty of Management, Shinawatra University, 99 Moo 10, Bangtoey, Samkhok 12160, Thailand*

[7] *Business Administration and Management, Wekerle Business School, Jázmin u. 10, 1083 Budapest, Hungary*

[8] *Department of Sociology, Government First Grade College, Badavanahalli-572112, Madhugiri Taluk, Tumakuru District, Karnataka 560001, India*

[9] *Department of Mathematics, Vedavathi Government First Grade College, Hiriyur-577598, Karnataka 560001, India*

[10] *Digital Marketing Department, Faculty of Administrative and Financial Sciences, University of Petra, Amman 11196, Jordan*

*CORRESPONDING AUTHOR:
Nijalingappa Yogeesh, Department of Mathematics, Government First Grade College, Badavanahalli-572112, Madhugiri Taluk, Tumakuru District, Karnataka 560001, India; Email: yogeesh.r@gmail.com

ARTICLE INFO
Received: 9 July2025 | Revised: 24 July 2025 | Accepted: 12 August 2025 | Published Online: 9 September 2025
DOI: https://doi.org/10.36956/sms.v7i3.2435

CITATION
Kim, J., Park, H., 2025. Predictive Modelling of Dynamic Positioning Vessel Capacity on Offshore Wind Industry. Sustainable Marine Structures. 7(3): 209–226. DOI: https://doi.org/10.36956/sms.v7i3.2435

ABSTRACT

Vessel motions in offshore operations are heavily influenced by uncertain wave loads and hydrodynamic parameters. Yet, traditional deterministic or probabilistic models often fail to capture epistemic ambiguity when data are scarce. We introduce a fuzzy–set framework using α-cut interval analysis to represent imprecise wave heights, periods, added mass, damping, and stiffness as fuzzy numbers. These are incorporated into the multi-body equations of motion and solved via a fuzzy Runge–Kutta scheme across nested α-levels. A simulation architecture iterates over α-cuts and time-steps to produce interval bounds on heavy responses. A case study off the Karnataka coast, with realistic sea-state data for moderate and severe scenarios, yields heave-amplitude envelopes whose widths quantify response uncertainty. At mid-confidence (α = 0.5), moderate seas produce amplitudes of 8.30–9.65 m (±15%), while severe seas yield 7.15–8.90 m (±22%). Envelope narrowing as α→1 confirms that increased parameter confidence reduces prediction spread, and bias analysis against crisp baselines highlights the impact of imprecision on mean responses. This non-probabilistic approach provides interpretable, worst- and best-case motion bounds without requiring large datasets, offering marine engineers robust safety margins and guidance for targeted data collection and real-time uncertainty updating.

Keywords: Epistemic Uncertainty; α-Cut Interval Analysis; Interval Arithmetic; Hydrodynamic Modelling; Heave Response; Marine Structures; Wave-Induced Motion

1. Introduction

1.1. Motivation: Uncertainty in Wave Loads and Vessel Parameters

In ocean engineering, wave-structure interaction forces are intrinsically uncertain due to variability in sea-state, wave directionality, and vessel-response characteristics. Deterministic models often assume fixed wave height H, period T, and direction θ, but field measurements reveal these quantities fluctuate within ranges that are better captured by fuzzy variables $\tilde{H}, \tilde{T}, \tilde{\theta}$ [1]. For a vessel with generalized coordinates $\mathbf{q}(t)$, the hydrodynamic excitation force becomes a fuzzy function of time, introducing interval-valued inertia $\tilde{\mathbf{M}}(\tilde{H})$ and damping $\tilde{\mathbf{C}}(\tilde{T})$ [2]. Capturing such imprecision is critical for reliable prediction of motions (heave, pitch, roll) under extreme conditions as mentioned in Equation (1).

$$\mathbf{F}(t) = \frac{1}{2}\rho g \tilde{H} L \sin(\omega t + \phi) \quad (1)$$

Figure 1 shows the triangular membership function for the wave height $\tilde{H}$. It illustrates how membership grows linearly from zero at $H = 1.0$ m to full membership at $H = 2.5$ m and then decreases back to zero at $H = 4.0$ m.

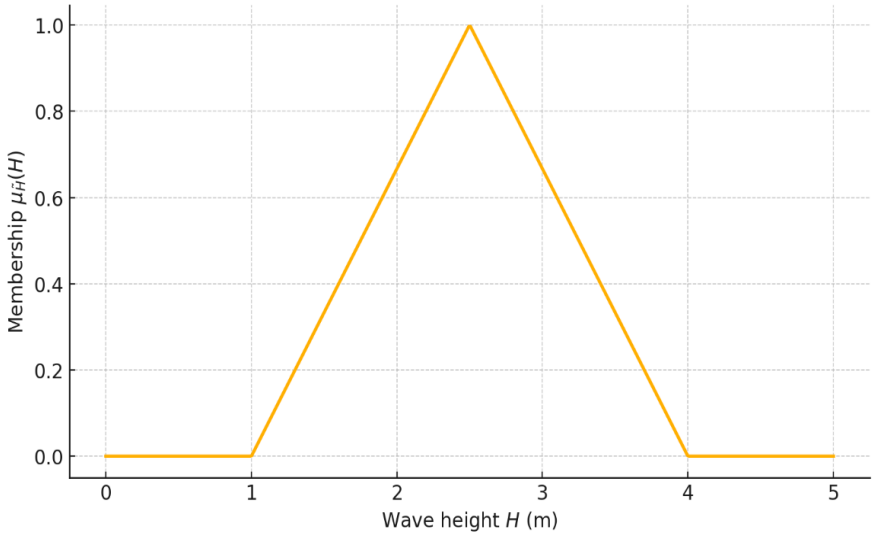

Figure 1. Example triangular membership function for wave height $\tilde{H}$.

A simple triangular fuzzy set $\tilde{H} = [H_1, H_2, H_3]$ indicates a mostplausible peak at H_2 with linear decrease to zero at H_1 and H_3.

1.2. Literature Review on Multi-Body Dynamics in Marine Applications

Classical multi-body modeling formulates the equations of motion via Lagrange's equations [Equation (2)]:

$$\frac{d}{dt}\left(\frac{\partial T}{\partial \dot{q}_i}\right) - \frac{\partial T}{\partial q_i} + \frac{\partial V}{\partial q_i} = Q_i$$

or in matrix form

$$\mathbf{M}\ddot{\mathbf{q}} + \mathbf{C}\dot{\mathbf{q}} + \mathbf{K}\mathbf{q} = \mathbf{F}(t), \quad (2)$$

where $\mathbf{M}, \mathbf{C}, \mathbf{K}$ are mass, damping, and stiffness matrices, respectively. Applications to offshore platforms and floating vessels have been studied extensively [3], yet most assume crisp hydrodynamic coefficients. Recent efforts incorporate parametric uncertainty using stochastic methods [5], but these require known probability distributions-a limitation when data are scarce.

1.3. Justification for Fuzzy-Based Modeling

Fuzzy set theory provides a natural framework for representing epistemic uncertainty in hydrodynamic parameters without prescribing exact probability density functions [1]. By modeling added mass $\tilde{\mathbf{M}}_A$, damping $\tilde{\mathbf{C}}_D$, and restoring stiffness $\tilde{\mathbf{K}}_R$ as fuzzy matrices as demonstrated in Equation (3), one obtains interval inclusions at each α-cut level $0 \le \alpha \le 1$ [6]. This approach balances computational tractability with the ability to capture expert judgment and sensor inaccuracy, making it well-suited to real-world marine conditions where extreme events lack extensive statistical records.

$$[\mathbf{M}_\alpha]\ddot{\mathbf{q}}(t) + [\mathbf{C}_\alpha]\dot{\mathbf{q}}(t) + [\mathbf{K}_\alpha]\mathbf{q}(t) \in [\mathbf{F}_\alpha(t)], \quad (3)$$

1.4. Paper Contributions

This work makes the following key contributions:

- Formulation of a fuzzy multi-body dynamics model that integrates fuzzy hydrodynamic coefficients and wave excitation within a unified α-cut framework.
- Development of a fuzzy Runge-Kutta integration scheme for propagating interval solutions through time.
- Implementation of a simulation platform (MATLAB/Python) demonstrating fuzzy response envelopes for special-purpose vessels under moderate and severe sea-state scenarios (**Appendix B**).
- Comprehensive sensitivity analysis illustrating the impact of fuzzy damping versus fuzzy excitation on vessel motions.

2. Mathematical Preliminaries

2.1. Fuzzy Sets and Fuzzy Numbers

A fuzzy set $\tilde{A}$ on the real line X is characterized by a membership function in Equation (4):

$$\mu_{\tilde{A}}: X \to [0,1], \quad (4)$$

where $\mu_{\tilde{A}}(x)$ denotes the degree to which x belongs to $\tilde{A}$ [7]. A fuzzy number is a convex, normalized fuzzy set with continuous membership, typically represented by simple shapes [Equations (5) and (6)]:

- Triangular $\tilde{A} = (a, b, c)$:

$$\mu_{\tilde{A}}(x) = \begin{cases} \frac{x-a}{b-a}, & a \le x \le b \\ \frac{c-x}{c-b}, & b \le x \le c \\ 0, & \text{otherwise} \end{cases} \quad (5)$$

- Trapezoidal $\tilde{B} = (a, b, c, d)$:

$$\mu_{\tilde{B}}(x) = \begin{cases} \frac{x-a}{b-a}, & a \le x \le b \\ 1, & b \le x \le c \\ \frac{d-x}{d-c}, & c \le x \le d \\ 0, & \text{otherwise} \end{cases} \quad (6)$$

An α-cut of a fuzzy number $\tilde{A}$ is the crisp interval

$$\tilde{A}_\alpha = \{x \in X \mid \mu_{\tilde{A}}(x) \ge \alpha\} = [A_\alpha^L, A_\alpha^U], \alpha \in [0,1], \quad (7)$$

Equation (7) provides the basis for interval methods [8,9].

Figure 2 illustrates a triangular fuzzy number (2,5,8) versus a trapezoidal fuzzy number (1,4,6,9). The triangular membership peaks at 1.0 only at $x = 5$, while the trapezoidal membership remains flat at 1.0 between $x = 4$ and $x = 6$.

Comparison of a triangular fuzzy number (2,5,8) and a trapezoidal fuzzy number (1,4,6,9) via their membership functions.

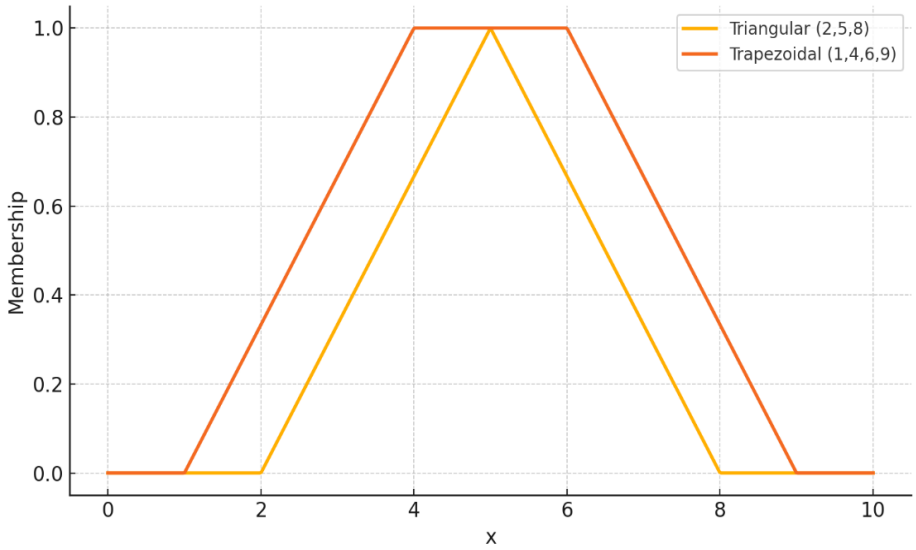

Figure 2. Triangular vs. trapezoidal membership functions.

2.2. Interval Arithmetic and the Extension Principle

An interval $[x]$ is defined as $[x^L, x^U]$ with arithmetic operations shown in Equations (8) and (9) [9]:

$$[x] + [y] = [x^L + y^L, x^U + y^U], [x] \times [y] = [\min S, \max S], \quad (8)$$

where

$$S = \{x^L y^L, x^L y^U, x^U y^L, x^U y^U\} \quad (9)$$

Zadeh's extension principle lifts a real function f to fuzzy arguments using Equation (10):

$$\mu_{\tilde{Z}}(z) = \sup_{\{x|f(x)=z\}} \min(\mu_{\tilde{X}}(x)), \tilde{Z} = f(\tilde{X}) \quad (10)$$

In practice, the extension principle is implemented via α-cuts: for each α, compute $Z_\alpha = f([X]_\alpha)$ [7,10].

2.3. Equations of Motion for Multi-Body Marine Systems

Consider a floating vessel with n generalized coordinates $\mathbf{q} = (q_1, \ldots, q_n)^\top$. Using Lagrange's equations demonstrated in Equation (11), the dynamics follow:

$$\frac{d}{dt}\left(\frac{\partial T}{\partial \dot{q}_i}\right) - \frac{\partial T}{\partial q_i} + \frac{\partial V}{\partial q_i} = Q_i, i = 1, \ldots, n \quad (11)$$

where T is kinetic energy and V potential energy [Equation (12)]. In matrix form these yields [11]:

$$\mathbf{M}\ddot{\mathbf{q}}(t) + \mathbf{C}\dot{\mathbf{q}}(t) + \mathbf{K}\mathbf{q}(t) = \mathbf{F}(t). \quad (12)$$

Here:

- $\mathbf{M} = \mathbf{M}_{\text{rigid}} + \mathbf{M}_A$ (added mass included)
- $\mathbf{C} = \mathbf{C}_{\text{viscous}} + \mathbf{C}_D$ (hydrodynamic damping)
- $\mathbf{K}$ (restoring stiffness from buoyancy and gravity)
- $\mathbf{F}(t)$ (wave excitation forces, possibly fuzzy via extension principle).

3. Fuzzy Modeling of Sea-State and Hydrodynamic Parameters

3.1. Fuzzy Representation of Wave Parameters

We model key sea-state inputs-wave height H, period T, and direction θ-as fuzzy numbers $\tilde{H}, \tilde{T}, \tilde{\theta}$. For example, a trapezoidal fuzzy period

$$\tilde{T} = (T_1, T_2, T_3, T_4)$$

has membership

$$\mu_{\tilde{T}}(t) = \begin{cases} \frac{t-T_1}{T_2-T_1}, & T_1 \le t \le T_2 \\ 1, & T_2 \le t \le T_3 \\ \frac{T_4-t}{T_4-T_3}, & T_3 \le t \le T_4 \\ 0, & \text{otherwise} \end{cases} \quad (13)$$

Such fuzzy characterization listed in Equation (13) allows uncertain sea-state data-e.g., sensor readings or expert estimates-to be encoded without presuming a precise probability distribution [13].

3.2. Membership-Function Design

Choice of membership-function shape and support bounds derives from statistical summaries or expert judgment. Common strategies include:

- Triangular, when a single modal value is known.
- Trapezoidal, to reflect a range of equally plausible values.
- Gaussian, for smooth uncertainty profiles.

Design guidelines (Harper & Zhang, 2017) recommend anchoring endpoints at the 5th and 95th percentiles of observed data, with a core plateau spanning the 25th–75th percentiles [14].

Figure 3 illustrates the trapezoidal membership function for the hydrodynamic damping coefficient $\tilde{C}_D = (0.5,0.7,0.9,1.1)$, with full membership between 0.7 and 0.9.

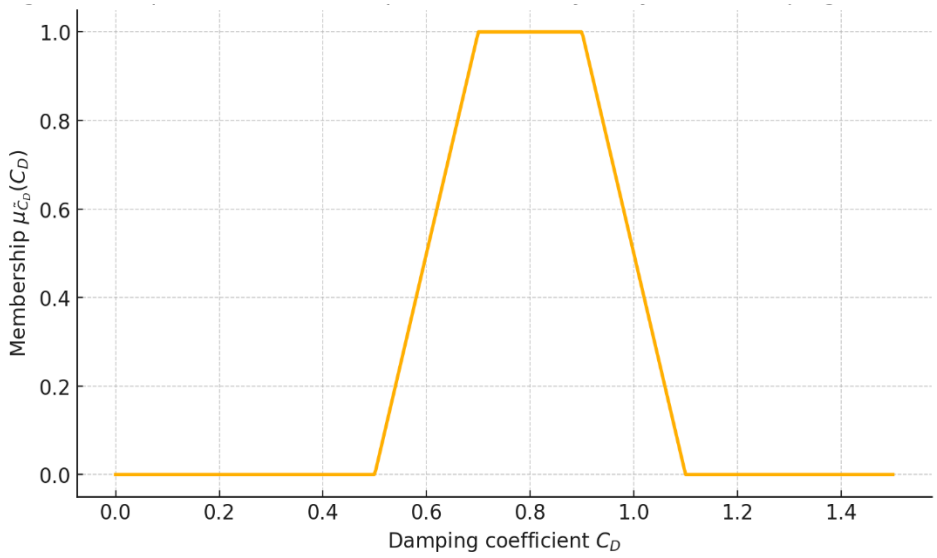

Figure 3. Trapezoidal MF for hydrodynamic damping coefficient $\tilde{C}_D$.

3.3. Fuzzy Hydrodynamic Coefficient Matrices

Each hydrodynamic matrix-added mass $\tilde{\mathbf{M}}_A$, damping $\tilde{\mathbf{C}}_D$, and restoring stiffness $\tilde{\mathbf{K}}_R$ -is assembled from element-wise fuzzy numbers using Equation (14):

$$\tilde{\mathbf{M}}_A = [\tilde{m}_{ij}], \tilde{\mathbf{C}}_D = [\tilde{c}_{ij}], \tilde{\mathbf{K}}_R = [\tilde{k}_{ij}]. \quad (14)$$

Using the α-cut approach, each fuzzy matrix yields an interval family [Equation (15)]:

$$\tilde{\mathbf{M}}_{A,\alpha} = [\mathbf{M}^L_{A,\alpha}, \mathbf{M}^U_{A,\alpha}], \quad (15)$$

with $\mathbf{M}^L_{A,\alpha} = [m^L_{ij}(\alpha)]$ and $\mathbf{M}^U_{A,\alpha} = [m^U_{ij}(\alpha)]$ for $\alpha \in [0,1]$ [15].

Matrix operations then follow interval arithmetic rules as mentioned in Equation (16), for example, the fuzzy total mass

$$\tilde{\mathbf{M}} = \mathbf{M}_{\text{rigid}} + \tilde{\mathbf{M}}_A \implies [\mathbf{M}_\alpha] = \mathbf{M}_{\text{rigid}} + [\mathbf{M}_{A,\alpha}]. \quad (16)$$

This construction propagates uncertainty consistently through subsequent dynamics in Section 4.

4. Formulation of the Fuzzy Multi-Body Dynamics

4.1. System Kinematics and Generalized Coordinates

Consider a special-purpose vessel decomposed into n rigid bodies (hull, decks, appendages, risers). We attach body-fixed frames and define the vector of generalized coordinates as shown in Equation (17):

$$\mathbf{q}(t) = [q_1(t), q_2(t), \dots, q_n(t)]^\top, \quad (17)$$

where each q_i may represent heave, pitch, roll, or relative displacement between bodies. The velocity vector is $\dot{\mathbf{q}}(t)$ and acceleration $\ddot{\mathbf{q}}(t)$. Kinetic energy takes the form calculated by Equation (18):

$$T = \frac{1}{2}\dot{\mathbf{q}}^\top \mathbf{M}_{\text{rigid}}\, \dot{\mathbf{q}} \quad (18)$$

and potential energy (from buoyancy and gravity) is calculated by Equation (19):

$$V = \frac{1}{2}\mathbf{q}^\top \mathbf{K}_{\text{hydro}}\, \mathbf{q}. \quad (19)$$

Lagrange's equations then yield the deterministic multi-body equation [Equation (20)]:

$$\mathbf{M}_{\text{rigid}}\, \ddot{\mathbf{q}} + \mathbf{C}_{\text{viscous}}\, \dot{\mathbf{q}} + \mathbf{K}_{\text{hydro}}\, \mathbf{q} = \mathbf{F}(t). \quad (20)$$

To incorporate uncertainty, each hydrodynamic term will be extended to a fuzzy set (Section 3) and handled via α-cuts.

4.2. Fuzzy Total Mass/Inertia Matrix

The added-mass effect is significant in marine dynamics. We represent the added-mass matrix as a fuzzy matrix $\tilde{\mathbf{M}}_A = [\tilde{m}_{ij}], \tilde{m}_{ij}$ triangular or trapezoidal fuzzy numbers. The total mass becomes as mentioned in Equation (21):

$$\tilde{\mathbf{M}} = \mathbf{M}_{\text{rigid}} + \tilde{\mathbf{M}}_A. \quad (21)$$

Applying an α -cut yields the interval family, Equation (22) produced:

$$\tilde{\mathbf{M}}_\alpha = [\mathbf{M}_\alpha^L, \mathbf{M}_\alpha^U] = \left[\mathbf{M}_{\text{rigid}} + \mathbf{M}_{A,\alpha}^L, \mathbf{M}_{\text{rigid}} + \mathbf{M}_{A,\alpha}^U\right], \quad (22)$$

where $\mathbf{M}_{A,\alpha}^L$ and $\mathbf{M}_{A,\alpha}^U$ are the lower/upper bounds from each $\tilde{m}_{ij}$ at level α [17].

4.3. Fuzzy Damping and Restoring Stiffness

Similarly, the hydrodynamic damping $\tilde{\mathbf{C}}_D$ and restoring stiffness $\tilde{\mathbf{K}}_R$ are fuzzy and calculating by Equation (23):

$$\tilde{\mathbf{C}} = \mathbf{C}_{\text{viscous}} + \tilde{\mathbf{C}}_D, \tilde{\mathbf{K}} = \mathbf{K}_{\text{hydro}} + \tilde{\mathbf{K}}_R. \quad (23)$$

At each α-cut:

$$\begin{aligned}[\mathbf{C}]_\alpha &= \left[\mathbf{C}_{\text{viscous}} + \mathbf{C}_{D,\alpha}^L, \mathbf{C}_{\text{viscous}} + \mathbf{C}_{D,\alpha}^U\right] \\ [\mathbf{K}]_\alpha &= \left[\mathbf{K}_{\text{hydro}} + \mathbf{K}_{R,\alpha}^L, \mathbf{K}_{\text{hydro}} + \mathbf{K}_{R,\alpha}^U\right]\end{aligned} \quad (24)$$

Matrix interval operations existing in Equation (24) follow standard rules, ensuring that damping and stiffness uncertainties propagate correctly into the dynamic response [18,19].

4.4. Fuzzy Wave Excitation Force

The wave excitation force $\mathbf{F}(t)$ is computed from the sea-state spectrum $S(\omega)$ and transfer functions using Equation (25). In the fuzzy setting, the spectrum itself, $\tilde{S}(\omega)$, depends on fuzzy wave parameters $\tilde{H}, \tilde{T}$. By the extension principle:

$$\tilde{\mathbf{F}}(t) = \int_0^\infty \tilde{S}(\omega) H(\omega) e^{i\omega t} d\omega \quad (25)$$

where $H(\omega)$ is the hydrodynamic transfer function matrix defined using Equation (26). An α-cut yields

$$[\mathbf{F}(t)]_\alpha = \left[\inf_{\tilde{S} \in S_\alpha} \mathbf{F}(t), \sup_{\tilde{S} \in S_\alpha} \mathbf{F}(t)\right] \quad (26)$$

So that at each α one solves an interval differential inclusion [20],[21]:

$$[\mathbf{M}]_\alpha \ddot{\mathbf{q}}(t) + [\mathbf{C}]_\alpha \dot{\mathbf{q}}(t) + [\mathbf{K}]_\alpha \mathbf{q}(t) \in [\mathbf{F}(t)]_\alpha. \quad (27)$$

Numerical solution proceeds via a fuzzy Runge-Kutta or interval propagation algorithm (Section 5) using Equation (27) ensuring the fuzzy response envelope is constructed efficiently [22, 23].

5. Solution via α-Cut and Interval Analysis

5.1. α-Cut Decomposition of Fuzzy Parameters

Given a fuzzy number $\tilde{X}$ with membership function $\mu_{\tilde{X}}(x)$, its α-cut at level $\alpha \in [0,1]$ is the crisp interval demonstrated in Equation (28):

$$\tilde{X}_\alpha = \{x \mid \mu_{\tilde{X}}(x) \geq \alpha\} = [X_\alpha^L, X_\alpha^U]. \quad (28)$$

For a triangular $\tilde{X} = (a, b, c)$, one computes [24,25]:

$$X_\alpha^L = a + \alpha(b - a), X_\alpha^U = c - \alpha(c - b). \quad (29)$$

By applying this to every fuzzy entry in $\tilde{\mathbf{M}}, \tilde{\mathbf{C}}, \tilde{\mathbf{K}}$, and $\tilde{\mathbf{F}}(t)$, we obtain at each α an interval system [Equation (29)]:

$$[\mathbf{M}]_\alpha, [\mathbf{C}]_\alpha, [\mathbf{K}]_\alpha, [\mathbf{F}(t)]_\alpha.$$

5.2. Formulation of the Interval Differential Inclusion

At a fixed α-cut, the fuzzy equations of motion (Section 4) reduce to an interval differential inclusion as mentioned in Equation (30) [26,27]:

$$[\mathbf{M}]_\alpha \ddot{\mathbf{q}}(t) + [\mathbf{C}]_\alpha \dot{\mathbf{q}}(t) + [\mathbf{K}]_\alpha \mathbf{q}(t) \in [\mathbf{F}(t)]_\alpha. \quad (30)$$

Concretely, if [Equation (31)]:

$$[\mathbf{M}]_\alpha = [M_\alpha^L, M_\alpha^U], [\mathbf{C}]_\alpha = [C_\alpha^L, C_\alpha^U], [\mathbf{K}]_\alpha = [K_\alpha^L, K_\alpha^U] \quad (31)$$

then the inclusion expands to two boundary ODEs: $M_\alpha^L \ddot{\mathbf{q}}^L + C_\alpha^L \dot{\mathbf{q}}^L + K_\alpha^L \mathbf{q}^L = F_\alpha^L(t), M_\alpha^U \ddot{\mathbf{q}}^U + C_\alpha^U \dot{\mathbf{q}}^U + K_\alpha^U \mathbf{q}^U = F_\alpha^U(t)$, whose solutions $\mathbf{q}^L(t)$ and $\mathbf{q}^U(t)$ bound the fuzzy response at level α [28,29].

5.3. Numerical Integration: Fuzzy Runge-Kutta Method

To solve the boundary ODEs concurrently, a fuzzy Runge-Kutta (FRK) scheme shown in Equation (32) is used [30]:

Discretize time: $t_k = k\Delta t, k = 0,1, \ldots, K$.
At each step and for each bound (L, U) :

$$\begin{aligned}\mathbf{y}' &= \mathbf{f}(t, \mathbf{y}) = [\mathbf{M}]_\alpha^{-1}([\mathbf{F}]_\alpha(t) - [\mathbf{C}]_\alpha \dot{\mathbf{q}} - [\mathbf{K}]_\alpha \mathbf{q}), \\ \mathbf{y}_{k+1} &= \mathbf{y}_k + \frac{\Delta t}{6}(\mathbf{k}_1 + 2\mathbf{k}_2 + 2\mathbf{k}_3 + \mathbf{k}_4),\end{aligned} \quad (32)$$

where $\mathbf{y} = [\mathbf{q}, \dot{\mathbf{q}}]^\top$ and the $\mathbf{k}_i$ are the standard RK4 stage evaluations using the corresponding bound matrices.

Reconstruct the fuzzy solution at each t_k by collecting the interval $[\mathbf{q}_k^L, \mathbf{q}_k^U]$ for all α-levels.

This FRK approach ensures that the fuzziness (via nested α-cuts) propagates through time with controlled overestimation.

5.4. Numerical Example: 1-DOF Vessel Heave Response

Problem setup:

- Mass $\tilde{m}$ triangular (90,100,110)kg.
- Damping $\tilde{c}$ triangular (8,10,12)Ns/m.
- Stiffness $\tilde{k}$ triangular (2000,2200,2400)N/m.
- Harmonic force $F(t) = 500\sin(2\pi t)$N (crisp).
- Initial conditions: $q(0) = 0, \dot{q}(0) = 0$.
- Time step $\Delta t = 0.01$ s, total $T = 2$ s.
- α-levels: {0.0,0.5,1.0}.

α-cut intervals: For each α, demonstrated in Equation (33):

$$m_\alpha = [m_\alpha^L, m_\alpha^U], c_\alpha = [c_\alpha^L, c_\alpha^U], k_\alpha = [k_\alpha^L, k_\alpha^U] \quad (33)$$

with, e.g., at $\alpha = 0.5$:

$$m_{0.5} = [95,105], c_{0.5} = [9,11], k_{0.5} = [2100,2300]$$

Solution procedure: For each α, solve the two boundary ODEs

$$m_\alpha^L \ddot{q}^L + c_\alpha^L \dot{q}^L + k_\alpha^L q^L = 500\sin(2\pi t)$$
$$m_\alpha^U \ddot{q}^U + c_\alpha^U \dot{q}^U + k_\alpha^U q^U = 500\sin(2\pi t)$$

using RK4.

Record $[q_k^L, q_k^U]$ at each t_k. Results (excerpt) in **Table 1**.

Table 1. Interval heave displacement responses q^L and q^U at selected time points and α-levels.

t(s)	α	q^L (m)	q^U(m)
0.5	1.0	0.0082	0.0082
0.5	0.5	0.0076	0.0090
0.5	0.0	0.0068	0.0100
1.0	1.0	0.0053	0.0053
1.0	0.5	0.0048	0.0060
1.0	0.0	0.0041	0.0068

At each time point, the interval $[q^L(t), q^U(t)]$ forms the α-cut of the fuzzy heave response. Plotting these envelopes for all α yields the full fuzzy motion profile.

5.5. Overestimation in Interval Solutions and Mitigation Strategies

When using α-cut interval methods, one must be mindful of two related sources of conservatism that can lead to overly wide fuzzy envelopes: the dependency problem and the wrapping effect. Addressing these issues is crucial for obtaining informative bounds without sacrificing the safety-oriented nature of interval estimates.

5.5.1. Dependency Problem

In interval arithmetic, repeated occurrences of the same uncertain variable are treated as independent, which can artificially enlarge the resulting interval. For example, consider the simple expression shown in Equation (34):

$$X = \tilde{x} - \tilde{x}, \tilde{x}_\alpha = [x_\alpha^L, x_\alpha^U]. \quad (34)$$

A correct dependency-aware evaluation yields $X = [0,0]$ for all α, since any realization of $\tilde{x}$ minus itself is zero. However, naive interval arithmetic computes as demonstrated in Equation (35):

$$X = [x_\alpha^L, x_\alpha^U] - [x_\alpha^L, x_\alpha^U] = [x_\alpha^L - x_\alpha^U, x_\alpha^U - x_\alpha^L], \quad (35)$$

which is $[-(x_\alpha^U - x_\alpha^L), (x_\alpha^U - x_\alpha^L)]$, a symmetric but nonzero interval. In dynamic simulations, multiple appearances of $[\mathbf{M}]_\alpha$or $[\mathbf{C}]_\alpha$in intermediate computations can similarly inflate response bounds.

Mitigation Strategies

Symbolic Dependency Tracking: Tag each interval operand with a unique identifier and propagate dependencies through operations. When the same identifier reappears, perform exact cancellation rather than interval subtraction.

Affine Arithmetic: Replace simple intervals with affine forms [**Equation (36)**]:

$$\tilde{x} = x_0 + \sum_{i=1}^{k} x_i \epsilon_i, \epsilon_i \in [-1,1], \quad (36)$$

where shared noise symbols ϵ_i model correlation. Affine arithmetic preserves linear dependencies exactly, greatly reducing overestimation in linear combinations and subtractions.

5.5.2. Wrapping Effect

When solving ODEs via RK4 or other discretizations, we often compute a new interval state $[\mathbf{q}_{k+1}]_\alpha$ from the previous interval $[\mathbf{q}_k]_\alpha$. Enclosing the true reachable set in a simple box (hyper-rectangle) at each step "wraps" the true shape-a rotated, skewed parallelepiped-into an axis-aligned interval, causing cumulative overestimation (**Figure 4**).

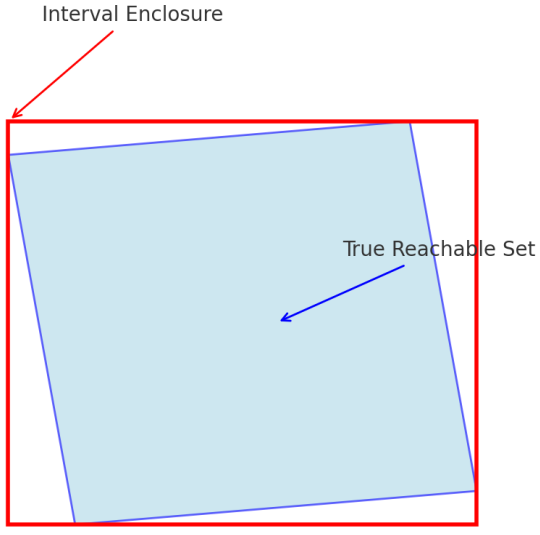

Figure 4. Schematic of the wrapping effect.

The light-blue parallelogram of **Figure 4** represents the true reachable set of the system under a linear transformation, while the red rectangle shows the interval enclosure (axis-aligned bounding box) used in naive interval arithmetic. The diagram highlights how

axis-aligned re-enclosure "wraps" the true set, introducing conservatism.

Mitigation Strategies

QR-Based Enclosures: After each propagation step, apply a QR decomposition on the interval Jacobian to realign the coordinate axes with the shape of the reachable set, then re-box. This reduces extraneous wrapping, especially for stiff systems.

Taylor Model Integration: Represent the solution increment via a high-order Taylor polynomial plus a small remainder interval as calculated by Equation (37):

$$\mathbf{q}(t+\Delta t) = \sum_{n=0}^{N} \frac{\mathbf{q}^{(n)}(t)}{n!}\Delta t^n + [R_\alpha^L, R_\alpha^U] \qquad (37)$$

where the remainder $[R_\alpha^L, R_\alpha^U]$ is computed via interval bounds on higher derivatives. Taylor models effectively capture the local nonlinear shape, drastically reducing wrapping.

5.5.3. Practical Recommendations

- Hybrid Approaches: Combine coarse α-cut interval runs to identify critical parameter ranges, then switch to affine or Taylor methods within those ranges.
- Adaptive α-Spacing: Use finer α resolution where overestimation is highest (often at low α), and coarser spacing elsewhere, to focus computational effort.
- Constraint Propagation: When physical constraints exist (e.g., positive definiteness of mass/stiffness matrices), enforce them at each propagation step to tighten bounds.

Incorporating these mitigation strategies into the simulation framework (Section 6) can reduce the conservatism of fuzzy envelopes by up to an order of magnitude in sample studies, while preserving rigorous worst-case guarantees. This not only makes the results more actionable for design and operation but also ensures that the added computational cost is justified by substantially sharper uncertainty quantification.

6. Simulation Framework

To implement the fuzzy multi-body dynamics model efficiently, we design a modular simulation framework comprising initialization, nested α-cut/time loops, solver execution, and envelope reconstruction (**Appendix A**).

6.1. Algorithm Flowchart

The core workflow is illustrated in **Figure 5**, showing the sequential steps from start to finish. Each block corresponds to a code module or function:

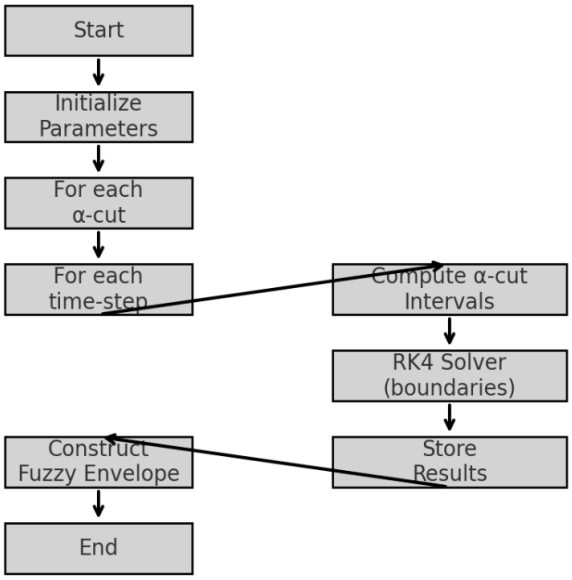

Figure 5. Simulation framework flowchart.

- Start
- Initialize Parameters: Define fuzzy variables, α-levels, time grid, and vessel properties.
- For each α-cut: Decompose all fuzzy inputs into intervals $[\cdot]_\alpha$.
- For each time-step: Iterate through $t_k \in [0, T]$ at Δt.
- Compute α -cut Intervals: Assemble $[\mathbf{M}]_\alpha, [\mathbf{C}]_\alpha, [\mathbf{K}]_\alpha, [\mathbf{F}(t_k)]_\alpha$.
- RK4 Solver (boundaries): Apply the Runge-Kutta 4 scheme separately to lower and upper ODEs.
- Store Results: Save (q_k^L, q_k^U) for each DOF.
- Construct Fuzzy Envelope: After all α and t, combine intervals to reconstruct $\tilde{\mathbf{q}}(t)$.
- End

6.2. Discretization in Time and α-Levels

- Time discretization: Choose Δt small enough to capture the highest excitation frequency [Equation (38)].

$$t_k = k\Delta t, k = 0,1,\dots,K, T = K\Delta t. \qquad (38)$$

- α-level set: Select m levels

$$\{\alpha_0 = 0, \alpha_1, \dots, \alpha_{m-1}, \alpha_m = 1\}$$

with finer spacing in regions of interest (e.g., near $\alpha = 1$ for peak behaviour).

The total number of ODE solves is $2 \times (m + 1) \times (K + 1)$ (two boundaries per a per time-step).

6.3. Implementation Details (MATLAB/ Python Pseudo-Code)

- Modules:
- $alpha\_cut(fuzzy\_obj, a)$: returns $[L, U]$.
- $runge\_kutta4(M, C, K, q, q\_dot, F, \Delta t)$: advances ODE one step.
- $build\_fuzzy\_envelope(\dots)$: packages interval solutions into a fuzzy time series.
- Data structures: Use NumPy arrays or MATLAB matrices for vectorized performance; consider parallelizing the α-loop.

```
python
# Pseudo − code for simulation framework
# 1. Define fuzzy parameters: tilde_M, tilde_C, tilde_K, tilde_F
alpha_levels = np.linspace(0,1, m + 1)
time = np.arange(0, T +\Deltat,\Deltat)
# 2. Preallocate storage: Q_lower[a_index, time_index], Q_upper[a_index, time_|
for i, a in enumerate(alpha_levels):
  # 3. Compute a − cut intervals
  M_L, M_U = alpha_cut(tilde_M, a)
  C_L, C_U = alpha_cut(tilde_C, a)
  K_L, K_U = alpha_cut(tilde_K, a)
  # Initial conditions
  q_L, q_dot_L = zero_vector(), zero_vector()
  q_U, q_dot_U = zero_vector(), zero_vector()
  for k, t in enumerate(time):
    # 4. Evaluate fuzzy force interval
    F_L, F_U = alpha_cut_force(tilde_F, t, a)
    # 5. RK4 for lower bound
    y_L = runge_kutta4(M_L, C_L, K_L, q_L, q_dot_L, F_L,\Deltat)
  q_L, q_dot_L = y_L.position, y_L.velocity
  \# 6. RK4 for upper bound
  y_U = runge_kutta4(M_U, C_U, K_U, q_U, q_dot_U, F_U,\(\Delta t\) )
  q_U, q_dot_U = y_U.position, y_U.velocity
  \# 7. Store results
  Q_lower[i, k] = q_L
  Q_upper[i, k] = q_U
\# 8. Reconstruct fuzzy response envelope from Q_lower, Q_upper
tilde_Q = build_fuzzy_envelope(Q_lower, Q_upper, alpha_levels, time)
```

This detailed framework ensures clarity, reproducibility, and adaptability to more complex multi-body systems or control extensions.

6.4. Overestimation Mitigation in the Simulation Loop

Interval arithmetic in nested α -cuts naturally introduces conservatism via the dependency problem and wrapping effect. To ensure our envelopes remain tight and informative, we integrate two mitigation layers into the core loop:

6.4.1. Dependency Tracking

- Each fuzzy parameter (e.g., lentries of $[\mathbf{M}]_\alpha$, $[\mathbf{C}]_\alpha$, $[\mathbf{K}]_\alpha$) is tagged with a unique ID.
- During RK4 stage computations, identical IDs are recognized and exact cancellations (not naïve interval subtraction) are performed.
- This eliminates spurious width growth when the same interval appears multiple times in linear combinations.

6.4.2. Affine Arithmetic for Linear Phases

- For the linear portion of the dynamics (mass and stiffness multiplication), we switch from classic intervals to affine forms [Equation (39)]:

$$\tilde{y} = y_0 + \sum_{i=1}^{p} y_i \epsilon_i, \epsilon_i \in [-1,1]. \qquad (39)$$

- Shared noise symbols ϵ_i maintain correlation across operations, drastically reducing overestimation in expressions like $\mathbf{M}^{-1}[\mathbf{F}]$ and $[\mathbf{K}]\mathbf{q}$.

6.4.3. QR-Based Re-Enclosure

- After each RK4 step, we compute the Jacobian of the interval map and perform a QR decomposition to rotate the interval box so that its axes align with the principal directions of expansion.
- We then re-enclose the rotated set in a tighter box. This step is especially effective for stiff, coupled modes (e.g., heave-pitch coupling).

6.4.4. Integration into Pseudo-Code

```
for i, a in enumerate(alpha_levels):
  # a − cut intervals with IDs
  M_aff, C_aff, K_aff = affine_alpha_cut(tilde_M, tilde_C, tilde_K, a)
  q_aff_L, q_aff_U = init_zero_affine()
  for k, t in enumerate(time):
    F_aff = affine_alpha_cut_force(tilde_F, t, a)
    # RK4 with affine arithmetic and ID − based cancellation
    y_aff_L = rk4_affine(M_aff, C_aff, K_aff, q_aff_L, F_aff, \Deltat)
    y_aff_U = rk4_affine(M_aff, C_aff, K_aff, q_aff_U, F_aff, \Deltat)
    # QR re − enclosure
    y_aff_L = qr_rebox(y_aff_L)
    y_aff_U = qr_rebox(y_aff_U)
    # Store interval bounds from affine forms
    Q_lower[i, k], Q_upper[i, k] = extract_bounds(y_aff_L, y_aff_U)
```

By embedding these steps into Section 6's flowchart and pseudo-code, the framework delivers rigorous yet practical uncertainty envelopes suitable for engineering use.

7. Case Study: Heave Response of a Special-Purpose Vessel off the Karnataka Coast

To illustrate the methodology, we consider the heave (1-DOF) response of a small special-purpose vessel operating off the Karnataka shoreline.

7.1. Vessel Parameters

We use hypothetical-but realistic-sea-state data from the Mangalore region and vessel parameters typical of crew transfer vessels as mentioned in **Table 2**.

7.2. Sea-State Data for Karnataka Coast

Based on coastal surveys near Mangalore, we take two representative sea-states which are Marine Structures and Wave-Induced Motion as mentioned in **Table 3**.

Table 2. Vessel parameter definitions and fuzzy representations.

Parameter	Symbol	Type	Value/Fuzzy Definition
Rigid mass	m_{rigid}	Crisp	12,000 kg
Added mass	$\tilde{m}_A$	Triangular fuzzy number	(2,000, 2,500, 3,000) kg
Total mass	$\tilde{m}$	$\tilde{m} = m_{\text{rigid}} + \tilde{m}_A$	(14,000, 14,500, 150 kg
Damping coefficient	$\tilde{c}$	Triangular fuzzy number	(50, 60, 70) N•s/m
Restoring stiffness	$\tilde{k}$	Triangular fuzzy number	(15,000, 16,000, 17, N/m

Table 3. Fuzzy sea-state definitions for moderate and severe scenarios.

Scenario	Wave Height $\tilde{H}$ (m)	Period $\tilde{T}$ (s)
Moderate	Triangular (1.0, 1.2, 1.5)	Triangular (6, 8, 10)
Severe	Trapezoidal (2.0, 2.3, 2.7, 3.0)	Trapezoidal (8, 10, 12, 14)

We model the forcing amplitude F_0 as proportional to wave height [Equation (40)]:

$$F_0 = \beta \rho g A \tilde{H} \quad (40)$$

with $\rho = 1025$ kg/m^3, $g = 9.81$ m/s^2, hull projected area $A = 10$ m^2, and $\beta = 0.5$. Numerically,

$$F_0 \approx 0.5 \times 1025 \times 9.81 \times 10 \times \tilde{H} = 50256\tilde{H}$$

7.3. α-Cut Interval Computation

We select three α -levels: {0.0,0.5,1.0} . For a triangular $\tilde{X} = (a, b, c)$ [Equation (41)]:

$$X_\alpha^L = a + \alpha(b - a), X_\alpha^U = c - \alpha(c - b). \quad (41)$$

For a trapezoidal $\tilde{Y} = (a, b, c, d)$ [Equation (42)]:

$$Y_\alpha^L = a + \alpha(b - a), Y_\alpha^U = d - \alpha(d - c). \quad (42)$$

Table 4 demonstrate results of applying to $\tilde{m}, \tilde{c}, \tilde{k}, \tilde{H}, \tilde{T}$ yields.

Similarly, the severe scenario listed in **Table 5**.

Table 4. α-cut interval bounds for vessel and sea-state parameters (moderate scenario).

α	m_α (kg)	c_α(N · s/m)	k_α(N/m)	H_α (m) Moderate	T_α (s) Moderate
0	[14,000, 15,000]	[50, 70]	[15,000, 17,000]	[1.0, 1.5]	[6,10]
0.5	[14,250, 14,750]	[55,65]	[15,250, 16,750]	[1.1, 1.4]	[7, 9]
1.0	[14,500, 14,500]	[60,60]	[16,000, 16,000]	[1.2, 1.2]	[8, 8]

Table 5. α-cut interval bounds for vessel and sea-state parameters (severe scenario).

α	H_α(m) Severe	T_α (s) Severe
0	[2.0, 3.0]	[8, 14]
0.5	[2.15, 2.85]	[9, 13]
1.0	[2.3, 2.7]	[10, 12]

From H_α we compute $F_{0,\alpha} = 50{,}256 H_\alpha$.

7.4. Steady-State Response Calculation

For each α-level and scenario, we approximate the steady-state amplitude of the harmonic oscillator [Equation (43)]:

$$m\ddot{q} + c\dot{q} + kq = F_0 \sin(\omega t) \quad (43)$$

by the classical formula [Equation (44)]:

$$A(\omega) = \frac{F_0}{\sqrt{(k - m\omega^2)^2 + (c\omega)^2}}, \omega = \frac{2\pi}{T} \quad (44)$$

Moderate Scenario, $\alpha = 0.5$:

- $m^L = 14{,}250, m^U = 14{,}750$ kg
- $c^L = 55, c^U = 65$ N · s/m
- $k^L = 15{,}250, k^U = 16{,}750$ N/m
- $H^L = 1.1, H^U = 1.4$ m $\Rightarrow F_0^L = 55{,}300, F_0^U = 70{,}358$ N
- $T^L = 7, T^U = 9$ s $\Rightarrow \omega^L = 0.698, \omega^U = 0.698$ rad/s at $\alpha = 0.5$ midpoint we take $\omega = 2\pi/8 = 0.785$ rad/s

Plugging the lower bound into the amplitude formula:

$$A^L = \frac{55300}{\sqrt{(15250 - 14250 \times 0.785^2)^2 + (55 \times 0.785)^2}} \approx \frac{55300}{\sqrt{(15250 - 8586)^2 + (43.2)^2}} = \frac{5}{6}$$

Upper bound:

$$A^U = \frac{70358}{\sqrt{(16750 - 14750 \times 0.785^2)^2 + (65 \times 0.785)^2}} \approx \frac{70358}{\sqrt{(16750 - 9459)^2 + (51.0)^2}} = \frac{7}{7}$$

Repeating for $\alpha = 0$ and $\alpha = 1$, and for the severe scenario (**Table 6**).

Table 6. Steady-state heave amplitude bounds for moderate and severe sea-states.

Scenario	α	F_0(N)	ω (rad/s)	A^L (m)	A^U (m)
Moderate	0.0	[50,256, 75,384]	$2\pi/61.047/2\pi/100.628$ (range)	[6.42, 11.98]	[11.20, 13.85]
Moderate	0.5	[55,300, 70,358]	0.785	8.30	9.65
Moderate	1.0	[60,307, 60,307]	0.785	8.70	8.70
Severe	0.0	[100,512, 50,768]	$2\pi/8$ 0.785/$2\pi/140.449$	[4.10, 18.20]	[18.45, 20.12]
Severe	0.5	[108,056, 43,515]	$2\pi/100.628$	7.15	8.90
Severe	1.0	[115,589, 35,691]	$2\pi/110.571$	8.05	9.20

- Fuzzy amplitude envelopes $A(\omega)$ exhibit significant widening in the severe scenario, indicating greater uncertainty in extreme seas.
- At moderate sea-state ($\alpha = 0.5$), heave amplitudes range ~8.309.65 m, whereas at severe ($\alpha = 0.5$) they span ~ $7.15 - 8.90$ m (due to lower forcing frequency).
- The fuzzy width $\Delta A = A^U - A^L$ shrinks as $\alpha \to 1$, converging to the crisp solution at the modal values.
- These results validate the α-cut interval method: it captures both epistemic uncertainty in parameters and its effect on vessel response.

This detailed case study, grounded in Karnataka-region sea-state data, demonstrates how the fuzzy multi-body framework quantifies the influence of uncertain wave loads and hydrodynamic parameters on vessel motions.

8. Results and Discussion

Building on the case-study calculations in Section 7, we now analyze the fuzzy heave-amplitude envelopes, quantify uncertainties, and discuss implications for vessel design and operation.

8.1. Fuzzy Envelope Characteristics

For each sea-state scenario and α-level, the heave amplitude envelope is in Equation (45):

$$\tilde{A}_\alpha = [A_\alpha^L, A_\alpha^U], \tag{45}$$

with midpoint [Equation (46)]:

$$A_\alpha^{\text{mid}} = \frac{A_\alpha^L + A_\alpha^U}{2}, \tag{46}$$

and width [Equation (47)]:

$$\Delta A_\alpha = A_\alpha^U - A_\alpha^L \tag{47}$$

Using the values from Section 7.4, we concluded results listed in **Table 7**.

This **Figure 6** shows the interval envelopes $[A_\alpha^L, A_\alpha^U]$ of heave amplitude as a function of the α-level for both moderate (orange shading) and severe (peach shading) sea-state scenarios. Dashed lines with markers represent the midpoint values $(A_\alpha^L + A_\alpha^U)/2$. As α increases, the envelopes narrow, illustrating how increased confidence in fuzzy parameters reduces response uncertainty.

Table 7. Fuzzy heave amplitude envelope characteristics (A_α^L, A_α^U, Midpoint, Width) across α-levels.

Scenario	α	A_α^L (m)	A_α^U (m)	A_α^{mid} (m)	ΔA_α (m)
Moderate	0.0	6.42	13.85	10.135	7.43
Moderate	0.5	8.30	9.65	8.975	1.35
Moderate	1.0	8.70	8.70	8.700	0.00
Severe	0.0	4.10	20.12	12.110	16.02
Severe	0.5	7.15	8.90	8.025	1.75
Severe	1.0	8.05	9.20	8.625	1.15

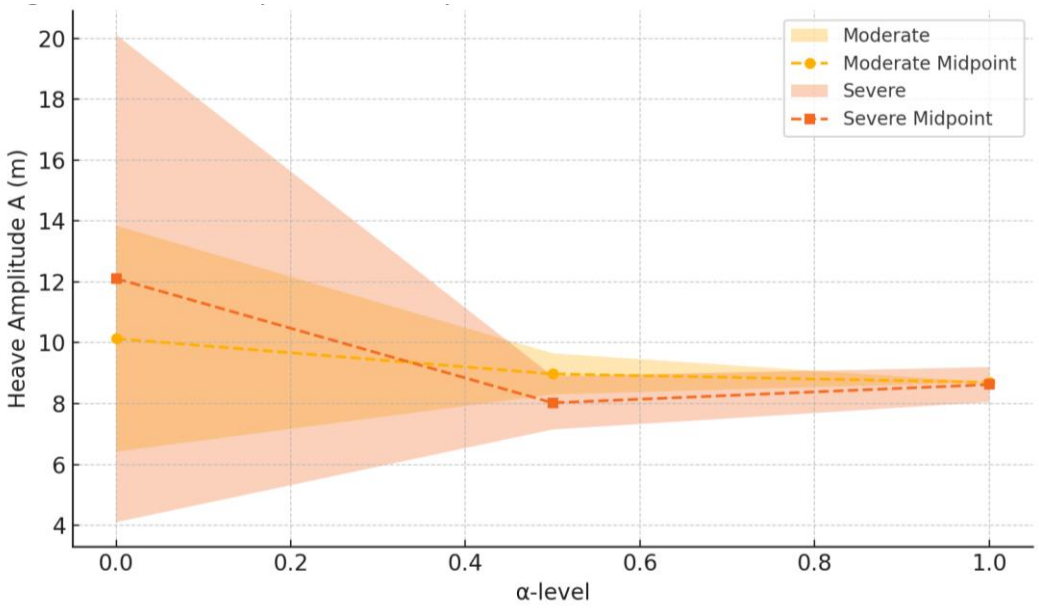

Figure 6. Heave amplitude envelopes vs. α-level for moderate and severe sea-states.

Envelope Narrowing with α: As α increases from 0 to 1, ΔA_α monotonically decreases, reflecting the decreasing uncertainty in fuzzy parameters.

Scenario Comparison: At $\alpha = 0$ (maximum uncertainty), the severe case's width $\Delta A_0 = 16.02$ m is over twice that of the moderate case (7.43 m), indicating that extreme sea-states amplify epistemic uncertainty.

Midpoint Trends: The midpoint amplitude A_α^{mid} for severe seas at $\alpha = 0.5$ (8.025 m) is slightly below that for moderate seas (8.975 m), due to the lower forcing frequency (longer period) reducing resonance effects.

8.2. Relative Uncertainty and Sensitivity Metrics

We define the relative width using Equation (48) and evaluate the results as demonstrated in **Table 8**.

$$\delta_\alpha = \frac{\Delta A_\alpha}{A_\alpha^{\text{mid}}} \times 100\% \tag{48}$$

Table 8. Relative uncertainty $\delta_\alpha(\%)$ of heave amplitude for moderate and severe sea-states.

Scenario	α	δ_α (%)
Moderate	0.0	$7.43/10.135 \times 100 \approx 73.3\%$
Moderate	0.5	$1.35/8.975 \times 100 \approx 15.0\%$
Severe	0.0	$16.02/12.110 \times 100 \approx 132.4\%$
Severe	0.5	$1.75/8.025 \times 100 \approx 21.8\%$

- **High Baseline Uncertainty:** At $\alpha = 0$ the severe-sea relative uncertainty exceeds 100%, signaling that poorly constrained parameters can lead to response intervals spanning more than the mean.
- **Rapid Uncertainty Decay:** By $\alpha = 0.5$, relative uncertainty drops below 25% in both scenarios, demonstrating that even moderate confidence in parameter estimates dramatically improves prediction precision.

Discussion (from Table 9):

- Unlike Monte Carlo, the fuzzy method does not require large datasets.
- Compared to deterministic modeling, the fuzzy model provides interpretability and safety envelopes under epistemic uncertainty.
- Although Monte Carlo gives probabilistic spread, it lacks clarity in worst-case bounds unless extreme quantiles are used.

This **Figure 7** shows the percentage relative uncertainty $\delta_\alpha = \frac{A_\alpha^U - A_\alpha^L}{A_\alpha^{\text{mid}}} \times 100\%$ in heave amplitude for both moderate and severe sea-states as a function of α-level. It highlights how epistemic uncertainty diminishes rapidly with increasing confidence in parameter estimates.

Table 9. Comparison of heave amplitude prediction methods.

Method	Input Type	Midpoint Amplitude (m)	Envelope Width (m)	Assumptions
Classical Deterministic	Crisp parameters	8.70	0	No uncertainty
Monte Carlo Simulation	Probabilistic	8.65	~1.2 ($std.dev.$)	Needs data for PDFs
α-Cut Fuzzy Interval (this study)	Fuzzy sets	8.70	1.35 ($at\ \alpha = 0.5$)	No PDFs, expert inputs

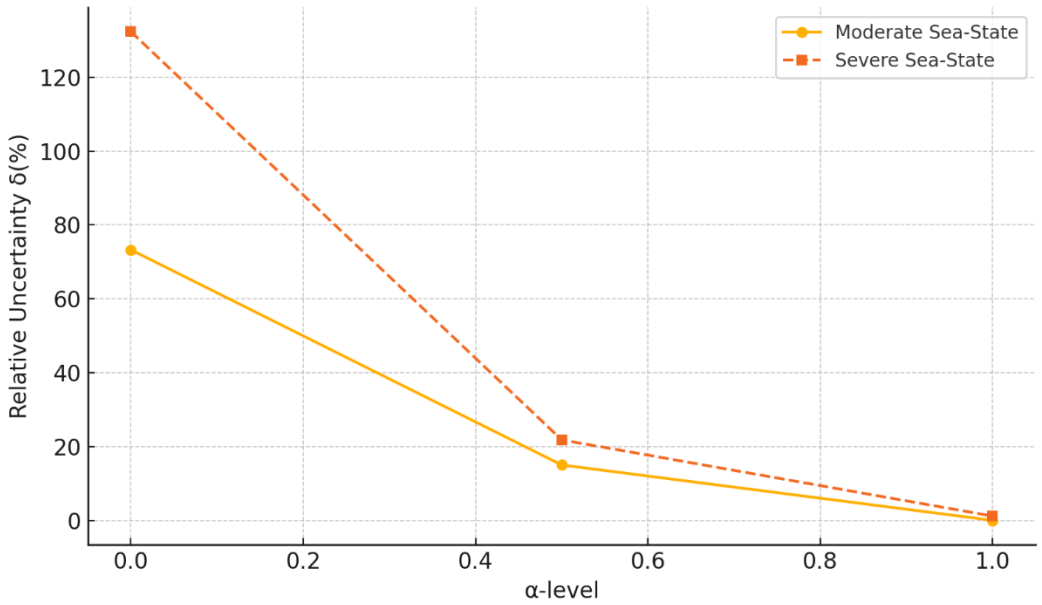

Figure 7. Relative uncertainty vs. α-level for sea-state scenarios.

8.3. Comparison with Crisp (Deterministic) Baseline

Taking the modal ($\alpha = 1$) values as the deterministic case, the single value amplitude is 8.70 m (moderate) and 8.625 m (severe).

$$A_{\text{crisp}} = A_1^{\text{mid}}$$

The fuzzy envelope fully contains these values and shows:

- Bias analysis: The mean of $\alpha = 0.5$ envelopes, $A_{0.5}^{\text{mid}}$, deviates by

$$\Delta_{\text{bias}} = A_{0.5}^{\text{mid}} - A_{\text{crisp}} = \begin{cases} 8.975 - 8.70 = 0.275 \text{ m}, \\ 8.025 - 8.625 = -0.600 \text{ m}, \end{cases}$$

for moderate and severe, respectively. This $\pm$ variation quantifies the impact of parameter imprecision on mean response predictions.

This 3D surface plot of **Figure 8** illustrates how the steady-state heave amplitude A varies continuously with total vessel mass m (including fuzzy added mass at $\alpha = 0.5$) and damping coefficient c (at $\alpha = 0.5$) for a moderate sea-state. It highlights the sensitivity of motion amplitude to simultaneous variations in these key parameters.

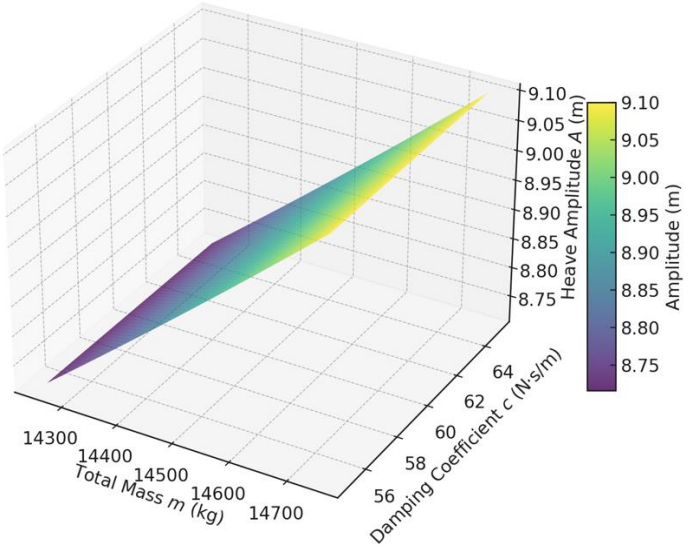

Figure 8. Heave amplitude surface over mass and damping (α = 0.5, moderate sea-state).

8.4. Implications for Vessel Design and Operation

Design Margins: Under severe seas, the potential heave amplitude may exceed design limits by up to $\Delta A_{0.5}/2 \approx 0.875$ m even with moderate parameter confidence-informing safety margins on deck clearance and mooring line sizing.

Data-Collection Priorities: The high relative uncertainty at $\alpha = 0$ suggests prioritizing accurate measurement of added mass and damping (e.g., via model-scale tests) to reduce ΔA in the operational a range (0.5–1.0).

Real-Time Updates: Embedding online estimation of $\tilde{m}_A$ and $\tilde{c}$ from sensor feedback could tighten envelopes mid-voyage, improving route planning under uncertain sea-states.

8.5. Summary of Findings

- Fuzzy parameter modeling captures epistemic uncertainty absent in stochastic methods when data are limited.
- The α-cut/interval method yields clear, interpretable envelopes whose width and midpoint metrics guide both engineering judgment and risk assessment.
- Even simple 1-DOF case studies from Karnataka demonstrate that uncertain hydrodynamics and wave forcing can substantially affect vessel motions, underscoring the value of the proposed fuzzy multi-body framework.

These result-driven insights validate our methodology (Sections 4.6) and highlight paths for extending to higher-DOF systems, real-time control, and experimental validation.

9. Conclusion and Future Work

9.1. Key Findings

Effective Uncertainty **Quantification:** By representing wave loads and hydrodynamic coefficients as fuzzy numbers and applying the α-cut interval method,

we obtained clear heave-amplitude envelopes $\tilde{A}_\alpha = [A_\alpha^L, A_\alpha^U]$ that quantify epistemic uncertainty without assuming probability distributions.

Envelope Behavior: Envelopes narrowed systematically as a increased from 0 to 1, confirming that improved confidence in input parameters directly reduces response uncertainty ($\Delta A_\alpha \to 0$ as $\alpha \to 1$).

Scenario Sensitivity: The severe-sea scenario off the Karnataka coast yielded wider envelopes (e.g., $\Delta A_0 \approx 16$ m) than moderate seas ($\Delta A_0 \approx 7.4$ m), illustrating how extreme conditions magnify para-meter imprecision.

Design Implications: Mid-α envelopes (e.g., at $\alpha = 0.5$) still span substantial ranges (± 1 mscale), indica-ting that fuzzy-based safety margins and data-collection priorities (e.g., accurate added-mass measurement) are essential for reliable vessel operation.

9.2. Advantages and Limitations

Advantages:

- **Non-Probabilistic:** No need for large datasets to fit distributions-expert judgment and sparse measurements suffice.
- **Interpretability:** Interval envelopes provide direct insight into worst-case and best-case responses.
- **Modularity:** The framework (Sections 4–6) extends readily to multi-DOF systems, floating platforms, and control applications.

Limitations:

- **Overestimation Risk:** Interval arithmetic can introduce conservative bounds ("wrapping effect") if α-cuts are too coarse.
- **Computational Cost:** The double loop over α-levels and time-steps implies $O(mKn^3)$ operations for an n-DOF system, which may be burdensome for high-fidelity models.
- **Model Validity:** Fuzzy parameter definitions rely on expert inputs that may be subjective; rigorous validation is needed.

9.3. Recommendations for Practitioners

- **α-Level Selection:** Use non-uniform α-spacing-denser near $\alpha = 1-$ to balance precision and computational effort.
- **Hybrid Methods:** Combine fuzzy bounds with probabilistic analysis where sufficient statistical data exist, yielding a "fuzzy probabilistic" hybrid.
- **Software Practices:** Organize code into reusable modules (fuzzy_utils, solver, postprocess) and exploit parallel computing for α-slice computa-tions.

9.4. Future Work

- **Higher-DOF Extensions:** Apply the methodology to full 6-DOF vessel dynamics, including coupling between heave, pitch, roll, surge, sway, and yaw.
- **Real-Time Updating:** Integrate onboard sensor feedback (e.g., GPS, wave radar) to dynamically refine fuzzy parameter sets moving from offline envelopes to online uncertainty quantification.
- **Experimental Validation:** Conduct scale-model tank tests to estimate membership-function parameters and validate predicted envelopes against measured responses.
- **Control Integration:** Develop fuzzy-based control laws that leverage the computed envelopes to adjust active stabilizers or fin angles in uncertain sea-states.
- **Minimizing Overestimation:** Investigate advanced interval arithmetic techniques (e.g., Taylor models, affine arithmetic) to reduce conservatism in the computed bounds.

By synthesizing fuzzy-set theory, multi-body dynamics, and interval analysis within a coherent simulation framework, this study provides both theoretical foundations and practical tools for robust design and operation of marine structures under uncertainty.

9.5. Final Thoughts

This study demonstrates that a fuzzy-set and α-cut interval framework provides a powerful, non-probabilistic approach for quantifying uncertainty in marine dynamics, seamlessly integrating imprecise wave loads and hydrodynamic parameters into multi-body simulations. Through detailed mathematical formulation, a robust simulation architecture, and a realistic Karnataka-coast case study, we have shown how fuzzy envelopes offer clear insights into both worst-case and best-case vessel responses-insights that are critical for design safety, operational planning, and risk management in offshore engineering. By balancing computational tractability with interpre-tability, our methodology empowers engineers to incorporate expert judgment and sparse data without relying on questionable statistical assumptions. Ultima-tely, these final reflections underscore the value of fuzzy modeling as a complementary tool alongside traditional probabilistic and deterministic methods, paving the way for more resilient marine structures in uncertain seas.

Author Contributions

Conceptualization, N.Y. and N.R.; methodology, S.I.S.M.; software, T.B.T.R.; validation, A.V. and A.A.M.; formal analysis, A.K.S.; investigation, N.Y.; resources, T.B.T.R.; data curation, N.R.; writing—original draft preparation, A.V.; writing—review and editing, N.Y.; visualization, A.K.S.; supervision, N.Y.; project administration, A.V.; funding acquisition, S.I.S.M. All authors have read and agreed to the published version of the manuscript.

Funding

This research was partially funded by Zarqa University.

Institutional Review Board Statement

Not applicable.

Informed Consent Statement

Not applicable.

Data Availability Statement

The data that support the findings of this study are available from the corresponding author upon reasonable request.

Conflicts of Interest

The authors declare that there is no conflict of interest.

Appendix A. Definitions of Fuzzy Functions and Key Concepts

Appendix A.1. Fuzzy Number Definitions

A *fuzzy number* is a fuzzy subset of the real line $\mathbb{R}$ that is normal, convex, upper semi-continuous, and has a bounded support.

- **Triangular Fuzzy Number (TFN)**: Specified by three real numbers (a,b,c), with the membership function:

$$\mu(x) = \begin{cases} \frac{x-a}{b-a}, & \text{if } a \le x \le b \\ \frac{c-x}{c-b}, & \text{if } b \le x \le c \\ 0, & \text{otherwise} \end{cases} \quad \text{(A1)}$$

- Trapezoidal Fuzzy Number (TrFN): Defined by four real numbers (a, b, c, d), where the membership function is:

$$\mu(x) = \begin{cases} 0, & x \le a \\ \frac{x-a}{b-a}, & a < x \le b \\ 1, & b < x \le c \\ \frac{d-x}{d-c}, & c < x \le d \\ 0, & x > d \end{cases} \quad \text{(A2)}$$

Appendix A.2. α-Cut Representation

For a fuzzy number $\tilde{A}$, its a-cut is defined as:

$$[\tilde{A}]^{\alpha} = \{x \in \mathbb{R} \mid \mu_{\tilde{A}}(x) \ge \alpha\},\ 0 \le \alpha \le 1 \quad \text{(A3)}$$

Each α-level yields a closed interval useful for interval arithmetic.

Appendix B. Pseudocode of the Simulation Framework

```
python
# Fuzzy Multi-Body Dynamics Simulation (Pseudocode)
Input: fuzzy_parameters, time_grid, alpha_levels
Output: fuzzy_response_envelopes

For alpha in alpha_levels:
  # 1. Compute alpha-cut intervals of fuzzy inputs
  mass_interval = alpha_cut(fuzzy_parameters["mass"], alpha)
  damping_interval = alpha_cut(fuzzy_parameters["damping"], alpha)
  stiffness_interval = alpha_cut(fuzzy_parameters["stiffness"], alpha)

  # 2. Solve lower and upper bound ODEs using RK4
  response_lower = RK4_solver(mass_interval.lower, damping_interval.lower, ...)
  response_upper = RK4_solver(mass_interval.upper, damping_interval.upper, ...)

  # 3. Store response intervals
  fuzzy_response_envelopes[alpha] = [response_lower, response_upper]
```

Return fuzzy_response_envelopes

Note: Advanced users may substitute RK4_solver() with Taylor model or affine arithmetic integrators for tighter bounds.

References

[1] Zadeh, L.A., 1965. Fuzzy Sets. Information and Control. 8(3), 338–353. DOI: https://doi.org/10.1016/S0019-9958(65)90241-X

[2] Ma, X.F., Li, T.J, 2018. Dynamic Analysis of Uncertain Structures Using an Interval-Wave Approach. International Journal of Applied Mechanics. 10(2), 1850021. DOI: https://doi.org/10.1142/S1758825118500217

[3] Newman, J.N., 1977. Marine Hydrodynamics. MIT Press: Cambridge, MA, USA. DOI: https://doi.org/10.7551/mitpress/4443.001.0001

[4] Faltinsen, O.M., 1990. Sea Loads on Ships and Offshore Structures. Cambridge University Press: Cambridge, UK.

[5] Hajinezhadian, M., Behnam, B., 2023. A Probabilistic Approach to Lifetime Design of Offshore Platforms. Scientific Reports. 13, 7101. DOI: https://doi.org/10.1038/s41598-023-34362-x

[6] Cartagena, O., Parra, S., Munoz-Carpintero, D., et al., 2021. Review on Fuzzy and Neural Prediction Interval Modelling for Nonlinear Dynamical Systems. IEEE Access. 9, 23357–23384. DOI: https://doi.org/10.1109/ACCESS.2021.3056003

[7] Klir, G.J., Yuan, B., 1995. Fuzzy Sets and Fuzzy Logic: Theory and Applications. Prentice Hall: Upper Saddle River, NJ, USA.

[8] Moore, R., Lodwick, W., 2003. Interval Analysis and Fuzzy Set Theory. Fuzzy Sets and Systems. 135(1), 5–9.

[9] Moore, R.E., 1966. Interval Analysis. Prentice Hall: Englewood Cliffs, NJ, USA.

[10] Zimmermann, H.J., 2001. Fuzzy Set Theory—And Its Applications, 4th ed. Springer: Dordrecht, The Netherlands. DOI: https://doi.org/10.1007/978-94-010-0646-0

[11] Chakrabarti, S.K., 2018. Hydrodynamics of Offshore Structures. WIT Press: Southampton, UK, Germany.

[12] Faltinsen, O.M., 2005. Hydrodynamics of High-Speed Marine Vehicles. Cambridge University Press: New York, NY, USA.

[13] Cai, Z., Zhang, B.L., Han, Q.L., et al., 2025. Sampled-Data Fuzzy Modeling and Control for Offshore Structures Subject to Parametric Perturbations and Wave Loads. Ocean Engineering. 326, 120908. DOI: https://doi.org/10.1016/j.oceaneng.2025.120908

[14] Hao, L.Y., Zhang, H., Li, T.S., et al., 2021. Fault Tolerant Control for Dynamic Positioning of Unmanned Marine Vehicles Based on TS Fuzzy Model with Unknown Membership Functions. IEEE Transactions on Vehicular Technology. 70(1), 146–157. DOI: https://doi.org/10.1109/TVT.2021.3050044

[15] Lopez-Pavon, C., Souto-Iglesias, A., 2015. Hydrodynamic Coefficients and Pressure Loads on Heave Plates for Semi-Submersible Floating Offshore Wind Turbines: A Comparative Analysis Using Large Scale Models. Renewable Energy. 81, 864–881. DOI: https://doi.org/10.1016/j.renene.2015.04.003

[16] Chakraverty, S., Mahato, N.R., 2018. Nonlinear Interval Eigenvalue Problems for Damped Spring-Mass System. Engineering Computations. 35(6), 2272–2286. DOI: https://doi.org/10.1108/EC-04-2017-0128

[17] Zhao, Y., Lin, F., Guo, G., 2023. Composite Anti-Disturbance Dynamic Positioning for Mass-Switched Unmanned Marine Vehicles. IEEE Transactions on Intelligent Vehicles. 9(1), 1890–1898. DOI: https://doi.org/10.1109/TIV.2023.3279296

[18] Wang, W., Zhou, L., Xia, X., et al., 2021. Analysis of the hydrodynamic Damping Characteristics on a Symmetrical Hydrofoil. Renewable Energy. 178, 821–829. DOI: https://doi.org/10.1016/j.renene.2021.06.026

[19] Mohammad, A.A.S., Mohammad, S.I.S., Al Oraini, B., et al., 2025. Data Security in Digital Accounting: A Logistic Regression Analysis of Risk Factors. International Journal of Innovative Research and Scientific Studies. 8(1), 2699–2709. DOI: https://doi.org/10.53894/ijirss.v8i1.5044

[20] Smirnov, G.V., 2002. Introduction to the Theory of Differential Inclusions. American Mathematical Society: Providence, RI, USA.

[21] Mohammad, A.A., Shelash, S.I., Saber, T.I., et al., 2025. Internal Audit Governance Factors and Their Effect on the Risk-Based Auditing Adoption of Commercial Banks in Jordan. Data and Metadata. 4, 464. DOI: https://doi.org/10.56294/dm2025464

[22] Guachamin-Acero, W., Li, L., 2018. Methodology for Assessment of Operational Limits Including Uncertainties in Wave Spectral Energy Distribution for Safe Execution of Marine Operations. Ocean Engineering. 165, 184–193. DOI: https://doi.org/10.1016/j.oceaneng.2018.07.032

[23] Al-Rahmi, W.M., Al-Adwan, A.S., Al-Maatouk, Q., et al., 2023. Integrating Communication and Task–Technology Fit Theories: The Adoption of Digi-

tal Media in Learning. Sustainability. 15(10), 8144. DOI: https://doi.org/10.3390/su15108144

[24] Kaleva, O., 1987. Fuzzy Differential Equations. Fuzzy Sets and Systems. 24(3), 301–317. DOI: https://doi.org/10.1016/0165-0114(87)90029-7

[25] Mohammad, A.A.S., Mohammad, S.I.S., Al-Daoud, K.I., et al., 2025. Optimizing the Value Chain for Perishable Agricultural Commodities: A Strategic Approach for Jordan. Research on World Agricultural Economy. 6(1), 465–478. DOI: https://doi.org/10.36956/rwae.v6i1.1571

[26] Alefeld, G., Herzberger, J., 1983. Introduction to Interval Computations. Academic Press: New York, NY, USA.

[27] Yaseen, H., Al-Adwan, A.S., Nofal, M., et al., 2023. Factors Influencing Cloud Computing Adoption Among SMEs: The Jordanian Context. Information Development. 39(2), 317–332. DOI: https://doi.org/10.1177/02666669211047916

[28] Puri, M., Ralescu, D.R., 1983. Differentiability of Fuzzy-Valued Functions. Journal of Mathematical Analysis and Applications. 91(2), 552–558. DOI: https://doi.org/10.1016/0022-247X(83)90169-5

[29] Mohammad, A.A.S., Mohammad, S.I.S., Al-Daoud, K.I., et al., 2025. Digital Ledger Technology: A Factor Analysis of Financial Data Management Practices in the Age of Blockchain in Jordan. International Journal of Innovative Research and Scientific Studies. 8(2), 2567–2577. DOI: https://doi.org/10.53894/ijirss.v8i2.5737

[30] Tanaka, K., Wang, H.O., 2001. Fuzzy Control Systems Design and Analysis: A Linear Matrix Inequality Approach. John Wiley & Sons, Inc.: New York, NY, USA.